U.S. National Library of Medicine
National Center for Biotechnology Information

NLM Citation: Leung K. ^{64}Cu-Tetraazacyclododecane-*N*,*N*′,*N*″,*N*‴-tetraacetic acid-quantum dot-c(Arg-Gly-Asp-D-Tyr-Lys). 2008 Mar 1 [Updated 2008 May 21]. In: Molecular Imaging and Contrast Agent Database (MICAD) [Internet]. Bethesda (MD): National Center for Biotechnology Information (US); 2004-2013.
Bookshelf URL: https://www.ncbi.nlm.nih.gov/books/

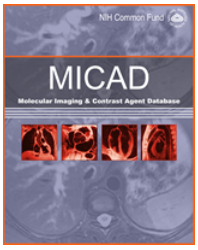

^{64}Cu-Tetraazacyclododecane-*N*,*N*′,*N*″,*N*‴-tetraacetic acid-quantum dot-c(Arg-Gly-Asp-D-Tyr-Lys)

^{64}Cu-DOTA-QD-c(RGDyK)

Kam Leung, PhD[1]

Created: March 1, 2008; Updated: May 21, 2008.

Chemical name:	^{64}Cu-Tetraazacyclododecane-*N*,*N*',*N*",*N*"'-tetraacetic acid-quantum dot-c(Arg-Gly-Asp-D-Tyr-Lys)	
Abbreviated name:	^{64}Cu-DOTA-QD-RGD, ^{64}Cu-DOTA-QD-c(RGDyK)	
Synonym:		
Agent Category:	Peptide	
Target:	Integrin $\alpha_v\beta_3$	
Target Category:	Receptor-ligand binding	
Method of detection:	Positron emission tomography (PET); optical, near-infrared (NIR) fluorescence	
Source of signal:	^{64}Cu and quantum dot	
Activation:	No	
Studies:	• *In vitro* • Rodents	Click on protein, nucleotide (RefSeq), and gene for more information about integrin $\alpha_v\beta_3$.

Background

[PubMed]

Optical fluorescence imaging is increasingly used to monitor biological functions of specific targets in small animals (1-3). However, the intrinsic fluorescence of biomolecules poses a problem when fluorophores that absorb visible light (350–700 nm) are used. Near-infrared (NIR) fluorescence (700–1,000 nm) detection avoids the background fluorescence interference of natural biomolecules, providing a high contrast between target and background tissues. NIR fluorophores have a wider dynamic range and minimal background as a result of reduced scattering compared with visible fluorescence detection. They also have high sensitivity, resulting from low fluorescence background, and high extinction coefficients, which provide high quantum yields. The NIR region is also compatible with solid-state optical components, such as diode lasers and silicon detectors. NIR

Author Affiliation: 1 National Center for Biotechnology Information, NLM, NIH, Bethesda, MD; Email: micad@ncbi.nlm.nih.gov.

fluorescence (NIRF) imaging is becoming a non-invasive alternative to radionuclide imaging in small animals (4, 5).

Fluorescent semiconductor quantum dots (QDs) are nanocrystals made of CdSe/CdTe-ZnS with radii of 1–10 nm (6-8). They can be tuned to emit light in a range of wavelengths by changing their sizes and composition, thus providing broad excitation profiles and high absorption coefficients. They have narrow and symmetric emission spectra with long excited-state lifetimes (20–50 ns) compared with fluorescent dyes (1–10 ns). QDs possess good quantum yields of 40–90% and high extinction coefficients, and they are more photo-stable than conventional organic dyes. They can be coated and capped with hydrophilic materials for additional conjugations with biomolecules, such as peptides, antibodies, nucleic acids, and small organic compounds, which are tested *in vitro* and *in vivo* (8-12). Although many cells have been labeled with QDs *in vitro* with little cytotoxicity, there are only limited studies of long-term toxicity of QDs in small animals (13-21), and little is known about the toxicity and the mechanisms of clearance and metabolism of QDs in humans.

Integrins are a family of heterodimeric, cell-surface glycoproteins that mediate diverse biological events involving cell–cell and cell–matrix interactions (22). Integrins comprise an α and a β subunit, and they are important for cell adhesion and signal transduction. The $\alpha_v\beta_3$ integrin is the most prominent receptor class, affecting tumor growth, tumor invasiveness, metastasis, tumor-induced angiogenesis, inflammation, osteoporosis, and rheumatoid arthritis (23-28). The $\alpha_v\beta_3$ integrin is strongly expressed on tumor cells and activated endothelial cells. In contrast, expression of $\alpha_v\beta_3$ integrin is weak on resting endothelial cells and on most normal tissues. The $\alpha_v\beta_3$ antagonists are being studied as anti-tumor and anti-angiogenic agents, and the agonists are being studied as angiogenic agents for coronary angiogenesis (27, 29, 30). A tripeptide sequence comprising Arg-Gly-Asp (RGD) has been identified as a recognition motif used by extracellular matrix proteins (vitronectin, fibrinogen, laminin, and collagen) to bind to a variety of integrins including $\alpha_v\beta_3$. Various radiolabeled cyclic RGD peptides have been introduced for tumor imaging and tumor angiogenesis (31). The multimodality probe ^{64}Cu-DOTA-QD-c(RGDyK) has been developed for PET and NIRF imaging of tumor vasculature to study *in vivo* biodistribution of the tracer in tumor-bearing mice (32). ^{64}Cu-DOTA-QD-c(RGDyK) has been shown to have a high accumulation in the tumor vasculature with little extravasation and a predominant liver and spleen accumulation.

Synthesis

[PubMed]

Commercially available QDs within amine-functionalized groups (emission, 705 nm; QD705, Invitrogen) were mixed with c(RGDyK)-4-maleimidobutyric acid *N*-hydroxysuccinimide ester and DOTA-*N*-hydroxysulfosuccinimide ester at room temperature for 1 h (32). The resulting DOTA-QD-RGD was purified with column chromatography. DOTA-QD was also prepared as a control. The molar ratio of DOTA to QD was estimated to be 28.2 for DOTA-QD-RGD and 118 for DOTA-QD. The number of RGD peptides was estimated to be 90 per QD nanoparticle. DOTA-QD-RGD or DOTA-QD (50 μg) was added to 74 MBq (2 mCi) of $^{64}CuCl_2$ in sodium acetate buffer (pH 6.5). The reaction mixture was incubated at 40°C for 1 h. The ^{64}Cu-labeling yield was >90% for both QD conjugates (n = 3).

In Vitro Studies: Testing in Cells and Tissues

[PubMed]

Cai et al. (32) performed competitive cell-binding assays using human glioblastoma U87MG tumor cells (expressing $\alpha_v\beta_3$). DOTA-QD-RGD inhibited the binding of ^{125}I-echistatin in a dose-dependent manner with a 50% inhibition concentration value of 3.88 nM, which was ~60-fold higher than c(RGDyK). Fluorescence microscopy showed that DOTA-QD had minimal binding to U87MG cells, whereas DOTA-QD-RGD (1 nM)

bound to the cell surface of U87MG cells. The DOTA-QD-RGD binding was inhibited by 1,000 nM c(RGDyK). On the other hand, DOTA-QD-RGD did not bind to $\alpha_v\beta_3$-negative C6 cells.

Animal Studies

Rodents

[PubMed]

Cai et al. (32) used a whole-body PET imaging system at 1, 5, 18, and 25 h to study the accumulation of ^{64}Cu-DOTA-QD-c(RGDyK) in mice bearing U87MG tumors. ^{64}Cu-DOTA-QD-c(RGDyK) (0.02 nmol/mouse) injected intravenously into nude mice (n = 3/group) bearing U87MG tumors (maximal tumor/muscle ratio = 4.1) showed that the liver, spleen, and lymph nodes were clearly visualized. Tumor accumulation of ^{64}Cu-DOTA-QD-c(RGDyK) was ~1% injected dose/gram (ID/g) at 1 h, 2.2% ID/g at 5 h, 4.0% ID/g at 18 h, and 4.3% ID/g at 25 h, distinctly higher than ^{64}Cu-DOTA-QD (<1% ID/g) at all time points. There was a marked intensity of signal in the liver (~50% ID/g) for both conjugates. *Ex vivo* PET imaging and NIRF imaging scans were performed on tissues harvested at 5 h. The liver, spleen, and bone marrow all had very strong signals, and the U87MG tumor exhibited significantly higher uptake than the heart, kidneys, and muscle. Both *in vivo* and *ex vivo* PET imaging data produced similar tissue/muscle ratios. The liver/muscle, spleen/muscle, bone/muscle, and kidney/muscle ratios were ~100:1, 30:1, 10:1, and 2:1, respectively. The U87MG tumor/muscle ratios for DOTA-QD-RGD and DOTA-QD were ~4:1 and 1:1, respectively. The liver/muscle, spleen/muscle, bone/muscle, kidney/muscle, and tumor/muscle ratios for NIRF imaging were ~100:1, 50:1, 40:1, 1:1, and 2:1, respectively. No blocking experiments were performed. Excellent linear correlation was observed between the signals measured with *in vivo* PET imaging and those measured with *ex vivo* NIRF imaging and tissue homogenate fluorescence (r^2 = 0.93). Histological examination of the tumor sections revealed that DOTA-QD-RGD targets primarily the tumor vasculature through an RGD–integrin $\alpha_v\beta_3$ interaction on the endothelial cells, with little extravasation.

Other Non-Primate Mammals

[PubMed]

No publication is currently available.

Non-Human Primates

[PubMed]

No publication is currently available.

Human Studies

[PubMed]

No publication is currently available.

NIH Support

R21 EB001785, R21 R01 CA119053, R21 CA121842, R21 CA102123, P50 CA114747, U54 CA119367, R24 CA93862

References

1. Achilefu S. Lighting up tumors with receptor-specific optical molecular probes. Technol Cancer Res Treat. 2004; **3** (4):393–409. PubMed PMID: 15270591.
2. Ntziachristos V., Bremer C., Weissleder R. Fluorescence imaging with near-infrared light: new technological advances that enable in vivo molecular imaging. Eur Radiol. 2003; **13** (1):195–208. PubMed PMID: 12541130.
3. Becker A., Hessenius C., Licha K., Ebert B., Sukowski U., Semmler W., Wiedenmann B., Grotzinger C. Receptor-targeted optical imaging of tumors with near-infrared fluorescent ligands. Nat Biotechnol. 2001; **19** (4):327–31. PubMed PMID: 11283589.
4. Robeson W., Dhawan V., Belakhlef A., Ma Y., Pillai V., Chaly T., Margouleff C., Bjelke D., Eidelberg D. Dosimetry of the dopamine transporter radioligand 18F-FPCIT in human subjects. J Nucl Med. 2003; **44** (6):961–6. PubMed PMID: 12791826.
5. Tung C.H. Fluorescent peptide probes for in vivo diagnostic imaging. Biopolymers. 2004; **76** (5):391–403. PubMed PMID: 15389488.
6. Zheng G., Li H., Yang K., Blessington D., Licha K., Lund-Katz S., Chance B., Glickson J.D. Tricarbocyanine cholesteryl laurates labeled LDL: new near infrared fluorescent probes (NIRFs) for monitoring tumors and gene therapy of familial hypercholesterolemia. Bioorg Med Chem Lett. 2002; **12** (11):1485–8. PubMed PMID: 12031325.
7. Gao X., Nie S. Quantum dot-encoded beads. Methods Mol Biol. 2005; **303** :61–71. PubMed PMID: 15923675.
8. Pinaud F., Michalet X., Bentolila L.A., Tsay J.M., Doose S., Li J.J., Iyer G., Weiss S. Advances in fluorescence imaging with quantum dot bio-probes. Biomaterials. 2006; **27** (9):1679–87. PubMed PMID: 16318871.
9. Alivisatos A.P., Gu W., Larabell C. Quantum dots as cellular probes. Annu Rev Biomed Eng. 2005; **7** :55–76. PubMed PMID: 16004566.
10. Hilger I., Leistner Y., Berndt A., Fritsche C., Haas K.M., Kosmehl H., Kaiser W.A. Near-infrared fluorescence imaging of HER-2 protein over-expression in tumour cells. Eur Radiol. 2004; **14** (6):1124–9. PubMed PMID: 15118831.
11. Medintz I.L., Uyeda H.T., Goldman E.R., Mattoussi H. Quantum dot bioconjugates for imaging, labelling and sensing. Nat Mater. 2005; **4** (6):435–46. PubMed PMID: 15928695.
12. Kabas J.S., Kisslo J., Flick C.L., Johnson S.H., Craig D.M., Stanley T.E., Smith P.K. Intraoperative perfusion contrast echocardiography. Initial experience during coronary artery bypass grafting. J Thorac Cardiovasc Surg. 1990; **99** (3):536–42. PubMed PMID: 2308372.
13. Akerman M.E., Chan W.C., Laakkonen P., Bhatia S.N., Ruoslahti E. Nanocrystal targeting in vivo. Proc Natl Acad Sci U S A. 2002; **99** (20):12617–21. PubMed PMID: 12235356.
14. Braydich-Stolle L., Hussain S., Schlager J.J., Hofmann M.C. In vitro cytotoxicity of nanoparticles in mammalian germline stem cells. Toxicol Sci. 2005; **88** (2):412–9. PubMed PMID: 16014736.
15. Kim S., Lim Y.T., Soltesz E.G., De Grand A.M., Lee J., Nakayama A., Parker J.A., Mihaljevic T., Laurence R.G., Dor D.M., Cohn L.H., Bawendi M.G., Frangioni J.V. Near-infrared fluorescent type II quantum dots for sentinel lymph node mapping. Nat Biotechnol. 2004; **22** (1):93–7. PubMed PMID: 14661026.
16. Gao X., Cui Y., Levenson R.M., Chung L.W., Nie S. In vivo cancer targeting and imaging with semiconductor quantum dots. Nat Biotechnol. 2004; **22** (8):969–76. PubMed PMID: 15258594.
17. Han M., Gao X., Su J.Z., Nie S. Quantum-dot-tagged microbeads for multiplexed optical coding of biomolecules. Nat Biotechnol. 2001; **19** (7):631–5. PubMed PMID: 11433273.
18. Lovric J., Bazzi H.S., Cuie Y., Fortin G.R., Winnik F.M., Maysinger D. Differences in subcellular distribution and toxicity of green and red emitting CdTe quantum dots. J Mol Med. 2005; **83** (5):377–85. PubMed PMID: 15688234.

19. Ohnishi S., Lomnes S.J., Laurence R.G., Gogbashian A., Mariani G., Frangioni J.V. Organic alternatives to quantum dots for intraoperative near-infrared fluorescent sentinel lymph node mapping. Mol Imaging. 2005; **4** (3):172–81. PubMed PMID: 16194449.
20. Shiohara A., Hoshino A., Hanaki K., Suzuki K., Yamamoto K. On the cyto-toxicity caused by quantum dots. Microbiol Immunol. 2004; **48** (9):669–75. PubMed PMID: 15383704.
21. Soltesz E.G., Kim S., Laurence R.G., DeGrand A.M., Parungo C.P., Dor D.M., Cohn L.H., Bawendi M.G., Frangioni J.V., Mihaljevic T. Intraoperative sentinel lymph node mapping of the lung using near-infrared fluorescent quantum dots. Ann Thorac Surg. 2005; **79** (1):269–77. PubMed PMID: 15620956.
22. Hynes R.O. Integrins: versatility, modulation, and signaling in cell adhesion. Cell. 1992; **69** (1):11–25. PubMed PMID: 1555235.
23. Jin H., Varner J. Integrins: roles in cancer development and as treatment targets. Br J Cancer. 2004; **90** (3):561–5. PubMed PMID: 14760364.
24. Varner J.A., Cheresh D.A. Tumor angiogenesis and the role of vascular cell integrin alphavbeta3. Important Adv Oncol. 1996.:69–87. PubMed PMID: 8791129.
25. Wilder R.L. Integrin alpha V beta 3 as a target for treatment of rheumatoid arthritis and related rheumatic diseases. Ann Rheum Dis. 2002; **61 Suppl 2**ii96–9. PubMed PMID: 12379637.
26. Grzesik W.J. Integrins and bone--cell adhesion and beyond. Arch Immunol Ther Exp (Warsz). 1997; **45** (4):271–5. PubMed PMID: 9523000.
27. Kumar C.C. Integrin alpha v beta 3 as a therapeutic target for blocking tumor-induced angiogenesis. Curr Drug Targets. 2003; **4** (2):123–31. PubMed PMID: 12558065.
28. Ruegg C., Dormond O., Foletti A. Suppression of tumor angiogenesis through the inhibition of integrin function and signaling in endothelial cells: which side to target? Endothelium. 2002; **9** (3):151–60. PubMed PMID: 12380640.
29. Kerr J.S., Mousa S.A., Slee A.M. Alpha(v)beta(3) integrin in angiogenesis and restenosis. Drug News Perspect. 2001; **14** (3):143–50. PubMed PMID: 12819820.
30. Mousa S.A. alphav Vitronectin receptors in vascular-mediated disorders. Med Res Rev. 2003; **23** (2):190–9. PubMed PMID: 12500288.
31. Haubner R., Wester H.J. Radiolabeled tracers for imaging of tumor angiogenesis and evaluation of anti-angiogenic therapies. Curr Pharm Des. 2004; **10** (13):1439–55. PubMed PMID: 15134568.
32. Cai W., Chen K., Li Z.B., Gambhir S.S., Chen X. Dual-function probe for PET and near-infrared fluorescence imaging of tumor vasculature. J Nucl Med. 2007; **48** (11):1862–70. PubMed PMID: 17942800.